Glyceraldehyde-3-phosphate dehydrogenase subunits A and B are essential to maintain photosynthetic efficiency

Andrew J. Simkin[1,2,*,+], Mohammed Alqurashi[2,+], Patricia E Lopez-Calcagno[2,3], Lauren R. Headland[2,4], Christine A. Raines[2]

[1] School of Biosciences, University of Kent, Canterbury, United Kingdom, CT2 7NJ, UK.
[2] Department of Biological Sciences, University of Essex, Wivenhoe Park, Colchester, CO4 3SQ, UK.
[3] School of Natural and Environmental Sciences, Newcastle University, Newcastle upon Tyne, NE1 7RU, UK
[4] School of Molecular Biosciences, University of Glasgow, Glasgow, G12 8QQ, UK

[+], These two authors corresponded equally to this work
*** To whom correspondence should be addressed.** E-mail: a.simkin@kent.ac.uk

Additional author emails:

m.khader@tu.edu.sa; Patricia.Lopez-Calcagno@newcastle.ac.uk; Lauren.Headland@glasgow.ac.uk; rainc@essex.ac.uk;

The author responsible for distribution of materials integral to the findings presented in this article in accordance with the policy described in the Instructions for Authors (https://academic.oup.com/plphys/pages/General-Instructions) is: Andrew J Simkin (a.simkin@kent.ac.uk)_.

Short title: Evaluation of GAPDH subunits A & B in Arabidopsis

One-sentence summary: A reduction in the level of either the GAPA or GAPB proteins in *Arabidopsis thaliana* results in significant reductions in photosynthetic efficiency and biomass. *In vivo* data is presented showing that the A_2B_2 form of GAPDH is necessary to maintain maximum photosynthetic capacity and growth.

ABSTRACT

In plants, glyceraldehyde-3-phosphate dehydrogenase (GAPDH; EC 1.2.1.12) reversibly converts 1,3-bisphosphoglycerate to glyceraldehyde-3-phosphate coupled with the reduction of NADPH to $NADP^+$. The GAPDH enzyme that functions in the Calvin Benson Cycle is assembled either from four glyceraldehyde-3-phosphate dehydrogenase A subunits (GAPA) proteins forming a homotetramer (A_4) or from two GAPA and two glyceraldehyde-3-phosphate dehydrogenase B subunit (GAPB) proteins forming a heterotetramer (A_2B_2). The relative importance of these two forms of GAPDH in determining the rate of photosynthesis is unknown. To address this question, we measured the photosynthetic rates of Arabidopsis (*Arabidopsis thaliana*) plants containing reduced amounts of the GAPDH A and B subunits individually and jointly, using T-DNA insertion lines of GAPA and GAPB and transgenic GAPA and GAPB plants with reduced levels of these proteins. Here we show that decreasing the levels of either the A or B subunits decreased the maximum efficiency of CO_2 fixation, plant growth, and final biomass. Finally, these data showed that the reduction in GAPA protein to 9% wild-type levels resulted in a 73% decrease in carbon assimilation rates. In contrast, eliminating GAPB protein resulted in a 40% reduction in assimilation rates. This work demonstrates that the GAPA homotetramer can compensate for the loss of GAPB, whereas GAPB alone cannot compensate fully for the loss of the GAPA subunit.

Key words: Glyceraldehyde-3-phosphate dehydrogenase; GAPDH; Photosynthesis; biomass

INTRODUCTION

In recent years there has been a focus to develop strategies to increase crop yields in order to feed the growing world population against the backdrop of climate change (IPCC, 2014; Pereira, 2017; IPCC, 2019; NASA, 2020). The photosynthetic capacity of a crop over the season determines the rate of growth and hence yield potential. A number of reports have now been published demonstrating that under glasshouse and field conditions improvements in photosynthesis, including the Calvin-Benson Cycle (CBC) can improve the productivity and yield of the plant (Driever et al., 2017; Kubis and Bar-Even, 2019; Simkin, 2019; Simkin et al., 2019; Burgess et al., 2022; De Souza et al., 2022; Raines et al., 2022). In the CBC, glyceraldehyde-3-phosphate dehydrogenase (GAPDH) catalyses the conversion of 1,3-bisphosphoglycerate to the triose phosphate, glyceraldehyde 3-phosphate (GAP) (Cséke and Buchanan, 1986). Previous work has shown that the antisense suppression of the GAPDH gene had no effect on the rate of CO_2 assimilation until GAPDH activity had decreased to 30-40% of WT levels (Price et al., 1995; Ruuska et al., 2000). However, more recently a study showed that overexpression of GAPDH in rice (*Oryza sativa*) resulted in increased photosynthetic CO_2 assimilation under elevated [CO_2] conditions (Suzuki et al., 2021), raising the possibility that GAPDH could be a target for future manipulations to improve photosynthesis.

The CBC GAPDH is highly regulated and in plants is comprised of two distinct subunits, the glyceraldehyde-3-phosphate dehydrogenase A subunits (GAPA) and the glyceraldehyde-3-phosphate dehydrogenase B subunits (GAPB) that function as either as a homotetramer A_4 or heterotetramer A_2B_2 (Cerff, 1979; Iadarola et al., 1983; Howard et al., 2011). The primary structures of these two subunits show considerable similarity and are produced from separate nuclear genes (*GapA1*, *GapA2* and *GapB*) (Cerff, 1995). The GAPA subunits share 92.6% identity and the major difference in the primary sequence between the GAPA and GAPB subunits is a C-terminal extension (CTE) on the GAPB, with substantial

similarity to the C-terminus of Chloroplast protein of 12 kDa (CP12) (Baalmann et al., 1996; Pohlmeyer et al., 1996), This CTE contains cysteine residues which have been shown to confer thioredoxin-mediated redox regulatory capacity onto the GAPDH A_2B_2 complex (Baalmann et al., 1996; Scheibe et al., 1996; Sparla et al., 2002; Marri et al., 2005; Fermani et al., 2007).

In the chloroplast of vascular plants, the predominant active form of GAPDH is believed to be the A_2B_2, however, leaves of many species contain other, less abundant forms of GAPDH including the A_4 form and the 2(A_2B_2) and 4(A_2B_2) multimers involved in deactivation of the enzyme (Wolosiuk and Buchanan, 1976; Scagliarini et al., 1998; Sparla et al., 2005; Fermani et al., 2007). The homotetramer A_4 form of GAPDH has been termed 'non-regulatory' ($GAPDH_N$), firstly because of the absence of the CTE identified in GAPB and secondly, it fails to aggregate into larger oligomers and the A_2B_2 regulatory form ($GAPDH_R$) (Scagliarini et al., 1998). In the absence of the CTE, $GAPDH_N$ is thought to be regulated by the formation of the CP12/GAPDH/PRK (Phosphoribulokinase) complex (Trost et al., 2006; Lopez-Calcagno et al., 2014). Although the regulation of the two tetramers of GAPDH are different, results of Scagliarini et al (1998) showed that the kinetic properties of $GAPDH_N$ are similar to $GAPDH_R$. The activity data for the GAPDH A_4 and the A_2B_2 showed that both of these isoforms have similar kinetic parameters, with a V_{max} (NADPH) of 130 and 114 μmol min^{-1} mg^{-1} respectively and a Km (BPGA) of 2.0 and 2.3 μM respectively. Based on these data it was proposed that that the B-subunits are mostly responsible for regulation of the enzyme (Sparla et al., 2005) and the A-subunits for catalytic activity (Scagliarini et al., 1998). Over and above the multimers of the A_2B_2 complex a further level of redox regulation of GAPDH activity occurs through the formation of a high molecular weight complex which includes the CBC enzyme PRK and the small regulatory protein CP12 (Howard et al., 2008; Carmo-Silva et al., 2011; Lopez-Calcagno et al., 2014; Lopez-Calcagno et al., 2017).

The A_4 homotetramer has been shown in spinach (*Spinacia oleracea*) chloroplast preparations to constitute 15–20% of the total GAPDH activity (Scagliarini et al., 1998). Howard et al. (2011) examined stromal extracts from dark-adapted leaves of species from Leguminosae (pea (*Pisum sativum* 'Onwards'), Medicago (*Medicago truncatula* 'Jemalong'), broad bean (*Vicia faba* 'The Sutton'), French bean (*Phaseolus vulgaris* 'Vilbel')), Solanaceae (potato (*Solanum tuberosum* 'Desiree'), tomato (*Solanum lycopersicon* 'Gardener's Delight'), and tobacco (*Nicotiana tabacum* 'Samson')), Amaranthaceae (spinach), and the Brassicaceae (Arabidopsis). This study revealed that the relative amounts of the A_2B_2 and the A_4 complexes vary among species. Whereas all species were found to accumulate the A_2B_2 heterotetramer, in contrast, in some plant species the A_4 tetramer was not detected (Howard et al., 2011). This raises the question of the role of the A_4 form for the activity of GAPDH in the CB cycle. To date the relative importance of the A_4 versus the A_2B_2 form of plastid GAPDH, in determining the rate of CO_2 assimilation, has not been elucidated. In this manuscript, to explore this question we have used insertion mutants in both the *GapB* and *GapA-1* genes together with transgenic lines where the relative amounts of the GAPA and GAPB proteins have been decreased individually.

RESULTS

Identification and analysis of Arabidopsis lines with reductions in GAPDH A and B transcript and protein levels

We identified T-DNA insertion mutants for *gapa-1* (SAIL_164_D01) and *gapb* (SAIL_308_A06) from The Arabidopsis Information Resource (TAIR) database (http://www.arabidopsis.org/). All T-DNA insertion sites were confirmed using PCR analysis of genomic DNA followed by sequencing of the T-DNA/gene junctions. The positions of the T-DNA inserts are presented in **Fig. 1**. Homozygous plants (identified by PCR) were used to

assess the effect of each T-DNA insertion on the expression of the GAPDH transcripts. RT-qPCR analysis confirmed that the transcript abundance encoding the GAPA subunit in the *gapa-1* mutant was reduced by approx. 45%, the remaining transcript being produced by the *gapa-2* gene (**Fig. 2A**). The transcript for the GAPB subunit in the *gapb* mutant was not detected in the T-DNA insertion line, evidencing the *gapb* mutant as a true knockout (KO) (**Fig. 2B**). In order to obtain additional independent mutant lines, GAPA and GAPB expression levels were downregulated using antisense constructs (Supplemental **Fig. S1, Fig. 2A and B**). Additionally, two GAPA co-suppressed lines were identified from plants transformed with a GAPA over-expression construct using the Arabidopsis sequence in the sense orientation (Supplemental **Fig. S1C**). In *GapA* co-suppressed transformants, we identified two lines with 5% (cA1) and 11% (cA2) of total *GapA* (*GapA-1* and *GapA-2*) transcript levels and antisense lines with 35% (aA1) and 11% (aA2) of *GapA* transcript (**Fig. 2A**). In anti-sense *GapB* transformants, we identified three lines with 11% (aB1), 15% (aB2) and 41% (aB2) levels of the *GapB* transcript (**Fig. 2B**). Western blot analysis of these mutant lines was used to determine changes in GAPDH protein levels, which showed a reduction in bands at 37.6 kDa representing GAPA and 47.7 kDa (**Fig. 2A and B**). In the GAPA1 insertion line and the GAPA1 antisense lines the level of the GAPA protein was reduced to 51-43% of the CN plants and in the GAPA co-supressed lines only 9% of the GAPA protein was detected (**Table 1**). In the GAPB insertion line no band was detected indicating the absence of the B subunit in this mutant (**Fig.2A**). The level of protein in the GAPB antisense lines was between 15 and 40% of the CN plants (**Fig.2B and Table 1**).

Chlorophyll fluorescence imaging reveals that PSII efficiency is maintained in plants showing a significant reduction in GAPA protein levels.

In order to explore the impact of a decrease in the subunits of the GAPDH enzyme on photosynthetic capacity, the quantum efficiency of PSII (F_q'/F_m'), chlorophyll *a* fluorescence was analysed (Baker, 2008; Murchie and Lawson, 2013). No significant decrease in F_q'/F_m' was observed in the *gapa-1* insertion line 164 which had a 45% reduction in *GapA* transcript levels and 46% reduction in GAPA protein or in the *gapb* insertion line 308 with no detectable level of the GAPB protein (**Table 1**). The GapA antisense lines, containing 46% of WT protein levels, maintained equivalent PSII photosynthetic efficiency to controls. GapB antisense lines also showed no significant differences in *Fq'/Fm'* consistent with the observed result in the *gapb* insertion line 308, suggesting that in the absence of GAPB, the presence of the GAPDH A subunit is sufficient to maintain the photosynthetic capacity of these plants.

A small decrease of 12% in F_q'/F_m' was found in the *GapA* co-suppressed lines that had the lowest level of GAPA protein (**Table 1**). To investigate further the impact of a combined reduction of both the GAPA and GAPB protein levels, double mutants *gapa-1/gapb* (164/308) were generated. Homozygous plants with insertions in both *gapa-1* (164) and *gapb* (308) were grown as described above. Interestingly, double mutants of *gapa-1*/*gapb* (164/308) showed a significant reduction in F_q'/F_m' suggesting that a GAPA protein level of 52% is insufficient to maintain photosynthetic efficiency in the absence of GAPB.

Photosynthetic CO_2 assimilation and electron transport rates are reduced in lines with reduced GAPDH protein level

To assess the impact on photosynthesis of changes in the levels of GAPDH protein, CO_2 assimilation rates were determined as a function of internal CO_2 concentration (C_i) (A/C_i' curve). Plants were grown in environmentally controlled chambers under short day conditions as described in materials and methods. The gas exchange measurements were made on mature leaves on plants six weeks after germination. A/C_i curves were determined for the *gapa-1*

insertion line (164), *gapb* insertion line (308), co-suppressed line of *GapA* (cA), *GapA* antisense line (aA), *GapB* antisense line (aB) and *gapa-1/gapb* crossed line (164/308) compared to the controls (CN) plants (**Fig. 3**). From these A/C_i curves, the maximum rate of CO_2 assimilation (A_{max}) in all mutant lines tested was shown to be significantly lower than for the CN plants. The plants with the lowest levels of the GAPA protein had the greatest decrease in assimilation rate (**Fig. 2A**), with maximum assimilation rates attained in these plants being approx. 27% of that observed in the CN (**Fig. 3A; Table 1**). Furthermore, in the *gapa-1* mutant (164), an approx. 50% reduction in GAPA protein levels resulted in a 40% reduction in maximum assimilation (**Fig. 3A**).

Plants with no detectable level of GAPB protein (**Fig 2B**) had a 30% decrease in assimilation rates compared to the 73% reduction observed in a line with 9% GAPA proteins (cA) (**Fig. 3B**). Finally, in line 164/308, representing the double mutant *gapa-1/gapb*, containing no GAPB protein and only 51% of the levels of GAPA protein, the assimilation rates are similar to the single *gapa-1* (164), and *gapb* (308) insertion mutants. This result suggests that the double mutant shows no cumulative impact on assimilation rates under these conditions as long as 51% GAPA protein remains (**Fig. 3C**).

Further analysis of the A/C_i curves using the equations published by von Caemmerer and Farquhar (1981) illustrated that the maximum rate of carboxylation by Rubisco (Vc_{max}) and maximum electron transport rate (J_{max}), were reduced in some lines (Sharkey et al., 2007; Sharkey, 2016) (Table 1). The results for Vc_{max} showed that lines with a reduction in GAPA displayed a significant decrease compared to CN. No significant difference in Vc_{max} was observed in plants with a reduction in GAPB.

Furthermore, the results showed that the lines with reductions in either GAPA or GAPB had a lower rate of photosynthetic electron transport (J_{max}), needed to sustain Ribulose 1,5-bisphosphate (RuBP) regeneration, when compared to control plants (Table 1). As previously

noted, the maximum rate of CO_2 assimilation (A_{max}) was significantly lower in all lines compared to CN, however, A_{max} was significantly lower in cA, where *GapA* transcript and GAPA protein levels were at the lowest levels. No significant differences in A_{max} were observed between the single mutants *gapa-1* (164) and *gapb* (308) compared to the double mutant *gapa-1/gapb* (164/308).

Growth and vegetative biomass are reduced in both GAPA and GAPB reduced lines

Growth analysis of GapA co-suppressed and insertion lines was carried out on homozygous plants grown in growth chambers at 22 °C under short day length (130 µmol m-2s-1 in an 8 h/16 h light/dark cycle) and relative humidity (RD) 50%. The growth rate of these plants was determined using image analysis of total leaf area over a period of 52 days from planting. Observations of the growth rates of *GapA* co-suppressed lines (cA), CN Columbia (Col-0), and the *gapa-1* and *gapb* insertion lines (164 and 308) showed a statistically significant reduction in all growth parameters (**Fig. 4;** Supplemental **Fig. S2**). The co-suppressed and insertion lines were shown to have a statistically significantly slower growth rate when compared to the CN plants at 40 days post planting (**Fig. 4A and B**). By 52 days post planting, this growth trend continued (**Fig. 4B**) and the final leaf area was reduced compared to controls (**Fig. 4B**).

A growth analysis of the *gapa-1* insertion mutant (164), the *GapA* co-suppressed (cA) and the *GapA* antisense lines (aA) showed a significant reduction in dry weight and leaf number (**Fig 5A**) compared to the CN. Significant reductions in the leaf number and final biomass were seen in the *gapb* insertion mutant (308) and *GapB* antisense lines was also observed when compared to CN (**Fig. 5B**). A comparative analysis of the single insertion mutants *gapa-1 and gapb* with the double mutants *gapa-1/gapb* showed that reduction in both the A and B subunits resulted in a greater decrease in leaf area, biomass and leaf number after 46 days of growth

(**Fig. ~~5C~~5B**), even in the absence of a larger decrease in assimilation rates observed in **Fig. 3C (see Table 1)**.

DISCUSSION

A reduction in GAPA protein levels inhibits CO_2 assimilation and reduces biomass yield

Previous research showed that a 60-70% reduction in GAPDH activity was needed to affect growth and development in tobacco (*N. tabacum* 'cv W38') antisense GAPDH lines and that no severe impact on photosynthesis was observed until levels were reduced to less than 35% of wild-type levels (Price et al., 1995). The results presented in this study clearly showed a slow growth phenotype in *A. thaliana* following reductions in GAPA protein levels by 50%. *GapA* co-suppressed lines, with more than a 90% reduction in *GapA* transcript levels and a barely detectable GAPA protein content showed the most statistically significant impact on photosynthetic efficiency (-73%) even with GAPB being present at wild-type levels. The principal form of GAPDH in plant chloroplast has been proposed to be the heterotetrameric A_2B_2. In some plants, including spinach, an A_4 homotetramer has also been detected representing up to 20% of total GAPDH activity (Scagliarini et al., 1998). This A_4 homotetramer was not detected in Arabidopsis by previous studies (Howard et al., 2011), providing evidence that under normal circumstances the A_2B_2 tetramer is the principal active form in Arabidopsis. In this study, plants showing an absence of GAPB protein in the *gapb* mutant lines-maintained photosynthesis rates at 66% of wild type levels suggesting that under conditions where GAPB is limiting, or absent, that the A_4 form of GAPDH can maintain photosynthesis.

Importantly, the work here also allowed a comparative analysis between plants with different levels of the GAPA and GAPB subunits under the same environmental conditions. When the *gapa-1* (164) and *gapb* (308) mutant lines were crossed to form the double mutant

gapa-1/gapb (164/308), the combined effects resulted in a cumulative reduction in biomass (-60%), which was significantly greater than the reductions observed in the *gapa-1* (-35%) or *gapb* (-16%) mutants alone. Interestingly, the assimilation rates for the *gapa-1/gapb* double mutant showed no further reductions compared to *gapa-1*, and *gapb* single mutants. Firstly, suggesting that GAPA, even though reduced in level, is able to maintain the assimilation rate even in the absence of GAPB and secondly, that the decrease in biomass observed in the double mutant may be due to impacts early in development leading to a cumulative effect on growth.

Recent reviews of the literature have shown that over-expressing of some CBC enzymes can lead to increases in photosynthesis and biomass and that a multi-target approach can result in cumulative yield gains in some plants (Simkin, 2019; Simkin et al., 2019; Raines, 2022). The co-overexpression of *GapA* and *GapB* in transgenic rice increased GAPDH activity to more than 3.2-fold of the wild-type levels; under elevated [CO_2], CO_2 assimilation increased by approximately 10% demonstrating that the overproduction of the chloroplast GAPDH proteins is effective at improving photosynthesis at least under elevated [CO_2]. However, under these conditions, no statistical significant differences in biomass were observed compared to wild-type plants, although a small increase in starch accumulation was observed. (Suzuki et al., 2021). In contrast, no statistical significant difference in CO_2 assimilation was observed in ambient [CO_2] (Suzuki et al., 2021). These results suggest that the manipulation of GAPDH activity may have more importance as atmospheric [CO_2] increases due to current climate change models where [CO_2] increases from 416 ppm to 550 by 2050 and 700 ppm by 2100 (Le Quéré et al., 2009; IPCC, 2019; NASA, 2020). Furthermore, given that no increase in growth rate or final biomass was observed at ambient [CO_2], increasing GAPDH may have more value in a multi-target approach, such as targeting additional CBC enzymes, photorespiratory elements and photosynthetic electron transport in combination with GAPDH in the same plants.

CONCLUSION

Our results have shown that both GAPA and GAPB are essential for normal growth and development in Arabidopsis plants and that the A_2B_2 form of the enzyme is required for maximum photosynthetic efficiency. The phenotypes described in this manuscript provide *in vivo* evidence of the relative importance of the individual subunits of the GAPDH complex on photosynthetic carbon assimilation. In this study we also show that the suppression of GAPA to almost undetectable levels resulted in a 73% decrease in carbon assimilation compared to 34% reduction in photosynthesis in the absence of GAPB providing direct evidence of the importance of GAPA in maintain photosynthetic capacity.

MATERIALS AND METHODS

Identification and analysis of T-DNA GAPDH mutants and production of double mutants

The *gapa-1* and *gapb* mutants in Arabidopsis (*Arabidopsis thaliana*) were identified in the Arabidopsis Information Resource (TAIR) database (*gapa-1*: SAIL_164_D01 and *gapb*: SAIL_308_A06). The mutant insertion sites were identified by PCR and the location of each T-DNA insertion was determined by sequencing the PCR products spanning the junction site (**Fig. 1**). The *GapA-1* was amplified with forward primers GapA1 Fwd (5'gagagcatgtgacataacggg'3) and reverse primer GapA1 Rev (5'accttaagcttggcctcagtc'3) in conjunction with primer Sail_LB3 (5'tagcatctgaatttcataaccaatctcgatacac'3). The *GapB* was amplified with forward primers GapB Fwd (5'cgacgatgtctcctctcagc'3) and reverse primer GapB Rev (5'gaccgggattcttgagacg'3) in conjunction with primer Sail_LB3. Double mutants *gapa-1/gapb* (164/308) was obtained by crossing homozygous plants of *gapa-1* (SAIL_164_D01) and *gapb* (SAIL_308_A06) and segregating the double homozygous plants.

Construct Generation

GAPA and GAPB antisense constructs

A partial-length coding sequence of glyceraldehyde-3-phosphate dehydrogenase A subunit (*GapA-1*: At3g26650) and the glyceraldehyde-3-phosphate dehydrogenase B subunit (*GapB*: At1g42970) were amplified by RT-PCR using primers AtGAPAf (5'cacctatcgaaggaaccggagtgtt'3) and AtGAPAr (5'tcctgtagatgttggaacaatg'3) and AtGAPBf (5'caccttgatggtaagctcatcaaagtt'3) and AtGAPBr (5'ggtgtaggagtgtgtggttgt'3) respectively. The resulting amplified products were cloned into pENTR/D (Invitrogen, UK) to make pENTR-GAPA1; pENTR-*antiGAPA* and pENTR-*antiGAPB.* The cDNA's were introduced into the pGWB2 gateway vector (Nakagawa et al., 2007; AB289765) by recombination from the pENTR/D vector to make pGWB2-AntiGAPA and pGWB2-AntiGAPB (Supplemental **Fig. S1**). cDNA are under transcriptional control of the 35s tobacco mosaic virus promoter, which directs constitutive high-level transcription of the transgene, and followed by the *nos* 3' terminator.

GAPA-1 sense constructs

Destination vector pGWPTS1 was generated as described in Simkin et al., (2017). The full-length coding sequencer of *GapA-1* was amplified using primers AtFwd (5'caccatggcttcggttactttctctgtcc'3) and AtRev (5'ttgatgaaatcacttccagttgttgg'3). The resulting amplified product was cloned into pENTR/D (Invitrogen, UK) to make pENTR-AtGAPA-1 and the sequence was verified and found to be identical. The full-length cDNA was introduced into destination vector pGWPTS1 by recombination from the pENTR/D vector to make pGWPTS1-AtGAPA-1 (PTS1-GAPA-1) (Supplemental **Fig. S1**). The transgene was under the control of the rbcS2B (1150bp; At5g38420) promoter. In this instance the expression of the cDNA was under transcriptional control of the Rubisco small subunit 2B (rbcS2B) promoter

(At5g38420), which directs high-level photosynthetic tissue specific transcription of the transgene and followed by the *nos* 3' terminator.

Generation of transgenic plants

The recombinant plasmid pGWB2-AntiGAPA, pGWB2-AntiGAPB and pGWPTS1-GAPA-1, were introduced into wild type Arabidopsis by floral dipping (Clough and Bent, 1998) using *Agrobacterium tumefaciens* GV3101. Positive transformants were regenerated on MS medium containing kanamycin (50mg L^{-1}). Kanamycin resistant primary transformants (T1 generation) with established root systems were transferred to soil and allowed to self-fertilize. Full details of pGWB2-AntiGAPA, pGWB2-AntiGAPB and PTS1-GAPA-1, construct assembly can be seen in the Supplemental **Fig. S1.**

Plant Growth Conditions

For experimental study, T3 progeny seeds from selected lines were germinated on soil in controlled environment chambers at an irradiance of 130 μmol photons m^{-2} s^{-1}, 22°C, relative humidity of 60%, in an 8h/16h square-wave photoperiod. Plants were sown randomly, and trays rotated daily. Leaf areas were calculated using standard photography and ImageJ software (imagej.nih.gov/ij). Wild type plants and null segregants (azygous) used in this study were evaluated independently. Once it was determined that no significant differences were observed between these two groups, wild type plants and null segregants were combined (null segregants from the transgenic lines verified by PCR for non-integration of the transgene) and used as a combined "control" group (CN) (Supplemental **Fig. S3**). Four leaf discs (0.6 cm diameter) from two individual leaves, were taken and immediately plunged into liquid nitrogen, and stored at -80°C for determination of transcript levels by qRT-PCR and protein content by western blot.

cDNA generation and RT-PCR

Total RNA was extracted from Arabidopsis leaf using the NucleoSpin® RNA Plant Kit (Macherey-Nagel, Fisher Scientific, UK). cDNA was synthesized using 1 µg total RNA in 20 µl using the oligo-dT primer according to the protocol in the RevertAid Reverse Transcriptase kit (Fermentas, Life Sciences, UK). cDNA was diluted 1 in 4 to a final concentration of 12.5ng μL^{-1}. For semi quantitative RT-PCR, 2 µL of RT reaction mixture (100 ng of RNA) in a total volume of 25 µL was used with DreamTaq DNA Polymerase (Thermo Fisher Scientific, UK) according to manufacturer's recommendations. For qPCR, the SensiFAST SYBR No-ROX Kit was used according to manufacturer's recommendations (Bioline Reagents Ltd., London, UK). GAPA-1 (At3g26650) and GAPA-2 (At1g12900) transcript were amplified using primers GAPA-F (5'atggttatgggagatgatatgg'3) and GAPA-R (5'ttattggcaacaatgtcagcc'3) and GAPB-F (5'ttcaggtgctctgatgtctctacc'3) and GAPB-R (5' tagccactaggtgagccaaatccacc'3) respectively.

Protein Extraction and Western Blotting

Total protein was extracted in extraction buffer (50 mM 4-(2-Hydroxyethyl)piperazine-1-ethanesulfonic acid (HEPES) pH 8.2, 5 mM MgCl2, 1 mM Ethylenediaminetetraacetic Acid Tetrasodium Salt (EDTA), 10% Glycerol, 0.1% Triton X-100, 2 mM Benzamidine, 2 mM Aminocaproic acid, 0.5 mM Phenylmethanesulfonyl fluoride (PMSF) and 10 mM DTT). Any insoluble material was removed by centrifugation at 14000 g for 10 min (4°C) and protein quantification was determined as previously described (Harrison et al., 1998; Simkin et al., 2017). Samples were loaded on an equal protein basis, separated using 12% (w/v) SDS-PAGE, transferred to polyvinylidene difluoride membrane, and probed using antibodies raised against GAPDH (Pohlmeyer et al., 1996). Proteins were detected using horseradish peroxidase conjugated to the secondary antibody and ECL chemiluminescence detection reagent (Amersham, Buckinghamshire, UK).

379

380 **Chlorophyll fluorescence imaging screening in seedlings**

381 Measurements were performed on 2-week-old Arabidopsis seedlings that had been
382 grown in a controlled environment chamber at 130 µmol $mol^{-2}s^{-1}$ PPFD and ambient
383 CO_2.Chlorophyll fluorescence parameters were obtained using a chlorophyll fluorescence (CF)
384 imaging system (Technologica, Colchester, UK (Barbagallo et al., 2003; von Caemmerer et al.,
385 2004)). The operating efficiency of photosystem two (PSII) photochemistry, F_q'/F_m', was
386 calculated from measurements of steady state fluorescence in the light (F') and maximum
387 fluorescence in the light (F_m') since $F_q'/F_m' = (F_m'-F')/F_m'$. Images of F' were taken when
388 fluorescence was stable at 130 µmol m^{-2} s^{-1} PPFD, whilst images of maximum fluorescence
389 were obtained after a saturating at 600 ms pulse of 6200 µmol m^{-2} s^{-1} PPFD (Oxborough and
390 Baker, 2000; Baker et al., 2001; Lawson et al., 2008; Simkin et al., 2017).

391

392 **Gas Exchange Measurements**

393 The response of net photosynthesis (A) to intracellular CO_2 (C_i) was measured using a
394 portable gas exchange system (CIRAS-1, PP Systems Ltd, Ayrshire, UK) as previously
395 described (Simkin et al., 2017). Leaves were illuminated with an integral red-blue LED light
396 source (PP systems Ltd, Ayrshire, UK) attached to the gas-exchange system, and light levels
397 were maintained at saturating photosynthetic photon flux density (PPFD) of 1000 µmol m^{-2} s^{-1}
398 for the duration of the A/C_i response curve. Measurements of A were made at ambient CO_2
399 concentration (Ca) at 400 µmol mol^{-1}, before Ca was decreased to 550, 350, 215, 60 µmol mol^{-1}
400 before returning to the initial value and increased to 740, 900, 1140, 1340, 1640 µmol mol^{-1}.
401 Measurements were recorded after A reached a new steady state (1-2 minutes). Leaf
402 temperature and vapour pressure deficit (VPD) were maintained at 25°C and 1 ± 0.2 kPa
403 respectively. The maximum rates of Rubisco- (Vc_{max}) and the maximum rate of electron

transport for RuBP regeneration (J_{max}) were determined and standardized to a leaf temperature of 25°C based on equations from von Caemmerer (1981), Bernacchi et al. (Bernacchi et al., 2001) and Sharkey (2016). All points below 200 ppm were assigned as rubisco-limited, points above 300 ppm as RuBP-regeneration limited as described (Sharkey, 2016).

Statistical Analysis

All statistical analyses were done by comparing ANOVA, using Sys-stat, University of Essex, UK. The differences between means were tested using the Post hoc Tukey test (SPSS, Chicago).

Accession numbers

Sequence data from this article can be found in the GenBank/EMBL data libraries under accession numbers_At3g26650 (NM113576) and At1g42970 (AY039961).

Supplemental Data

Supplemental Figure S1. Schematic representation constructs used for floral dipping.

Supplemental Figure S2. Original photos for Figure 4. Growth analysis of control and experimental lines grown in low light.

Supplemental Figure S3. Growth analysis of non-transformed (WT) and Azygous (Azy) experimental lines grown in low light.

Funding information

A.J.S, P.E.L.C and L.H were supported by BBSRC (Grant: BB/J004138/1 awarded to C.A.R). M.A was funded by the Saudi Arabian Government and by the University of Essex Research

Incentive Scheme to C.A.R. A.J.S is supported by the Growing Kent and Medway Program, UK; Ref 107139.

ACKNOWLEDGMENTS

We thank Phillip A. Davey (University of Essex, UK) for help with gas exchange and Tracy Lawson for help with SigmaPlot.

Author Contributions: A.J.S and M.A generated transgenic plants and performed molecular and biochemical experiments and carried out plant phenotypic and growth analysis. P.E.L.C and L.R.H screened and identified GPADH insertion mutants and assisted in experimental design. M.A performed gas exchange measurement on Arabidopsis. A.J.S and M.A carried out data analysis on their respective contributions. C.A.R conceived and designed the research and C.A.R and A.J.S supervised the research. C.A.R, A.J.S wrote the manuscript with input from all authors.

Tables

Table I. *Maximum electron transport rate (J_{max}), the maximum rate of carboxylation by Rubisco (Vc_{max}) and maximum assimilation (A_{max}) in wild-type and GAPDH lines.*

Plants were grown in short days at 130 µmol m^{-2} s^{-1} light intensity, 8 h light/16 h dark cycle. Values represent 4-6 plants independent lines (6-8 plants) for group. A_{max} and J_{max} derived from A/C_i response curves shown in Figure 3 using the equations published by von Caemmerer and Farquhar (1981) using the spreadsheet provided by Sharkey, (2016). ND = not detected. Statistical differences are shown in boldface ($P < 0.05$). SE are shown. WT = plants containing Wild Type levels of the transcript and protein subunit. Protein quantities are shown in italics.

Line	**Relative % *GapA* transcript and *protein***	**Relative % *GapB* transcript and *protein***	***Fq'/Fm'* 600 µmol m^{-2} s^{-1}**	***J_{max}***	***Vc_{max}***	***A_{max}***
CN	WT	WT	0.478 +/- 0.014	145.5 +/- 15.75	55.1 +/- 5.2	28.3 +/- 1.15
164	**55.2 +/- 15.5**	WT	0.479 +/- 0.004	**89.0 +/- 11.12**	**40.2 +/- 5.62**	**16.2 +/- 2.71**
	51.6 +/- 1.9					
cA	**9.4 +/- 4.4**	WT	**0.420 +/- 0.014**	**51.9 +/- 4.41**	**37.6 +/- 3.19**	**7.67 +/- 0.91**
	9.1 +/- 3.7					
aA	**23.3 +/- 11.8**	WT	0.449 +/- 0.006	**119.7 +/- 7.90**	**40.2 +/- 2.67**	**23.4 +/- 1.38**
	43.6 +/-5.1					
308	WT	**ND**	0.469 +/- 0.003	**101.8 +/- 8.91**	56.4 +/- 1.12	**18.8 +/- 2.27**
aB	WT	**22.3 +/- 9.34**	0.453 +/- 0.004	**110.5 +/- 17.12**	52.3 +/- 5.92	**18.2 +/- 2.34**
		26.1 +/- 13.8				*******
164/	**55.2 +/- 15.5**	**ND**	**0.450 +/- 0.012**	**101.1 +/- 4.44**	**38.4 +/- 3.49**	**20.1 +- 0.54**
308	***51.6 +/- 1.9***					

CN = control. *gapa-1* insertion (164); *gapb* insertion (308); co-supressed GapA (cA); antisense GapA (aA); antisense GapB (aB);

458 **Figure Legends**

Figure 1

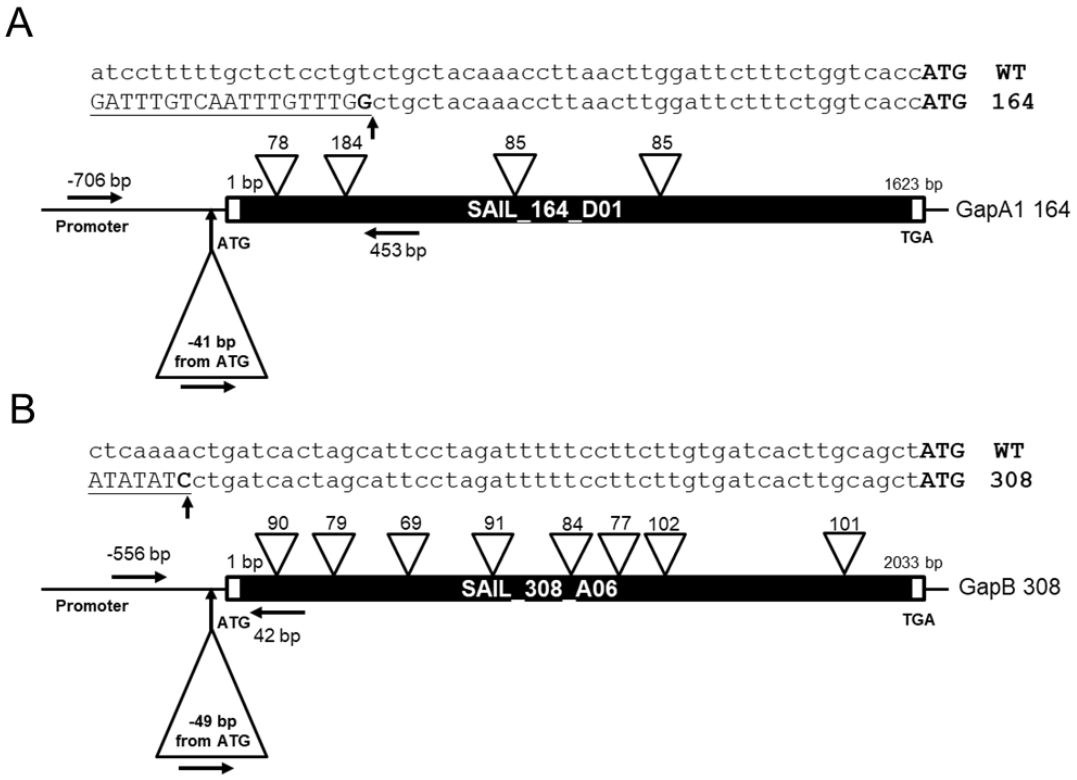

459

460 **Figure 1. Molecular analysis of homozygous GAPDH T-DNA insertion mutants.** Structure
461 of the two GAPDH genes and the location of T-DNA insertions in the (A) *gapa-1* (At3g26650;
462 SAIL_164_D01) and (B) *gapb* (At1g42970; SAIL_308_A06) mutants. Protein-coding exons
463 are represented by black and intron locations are displayed as inverted white triangles above
464 the coding sequence. Location of genomic PCR-screening primers are shown by black arrows
465 on each gene model. T-DNA insertion sites are indicated by triangles below the sequence and
466 the precise position is given as the number of base pairs from the ATG. ATG, translation
467 initiation codon; TGA, translation termination codon. Bolded G (Panel A) and C (Panel B)
468 indicate the point of sequence insertion into the promoter region of the SAIL_164_D01 and
469 SAIL_308_A06 mutants.

470

471

Figure 2

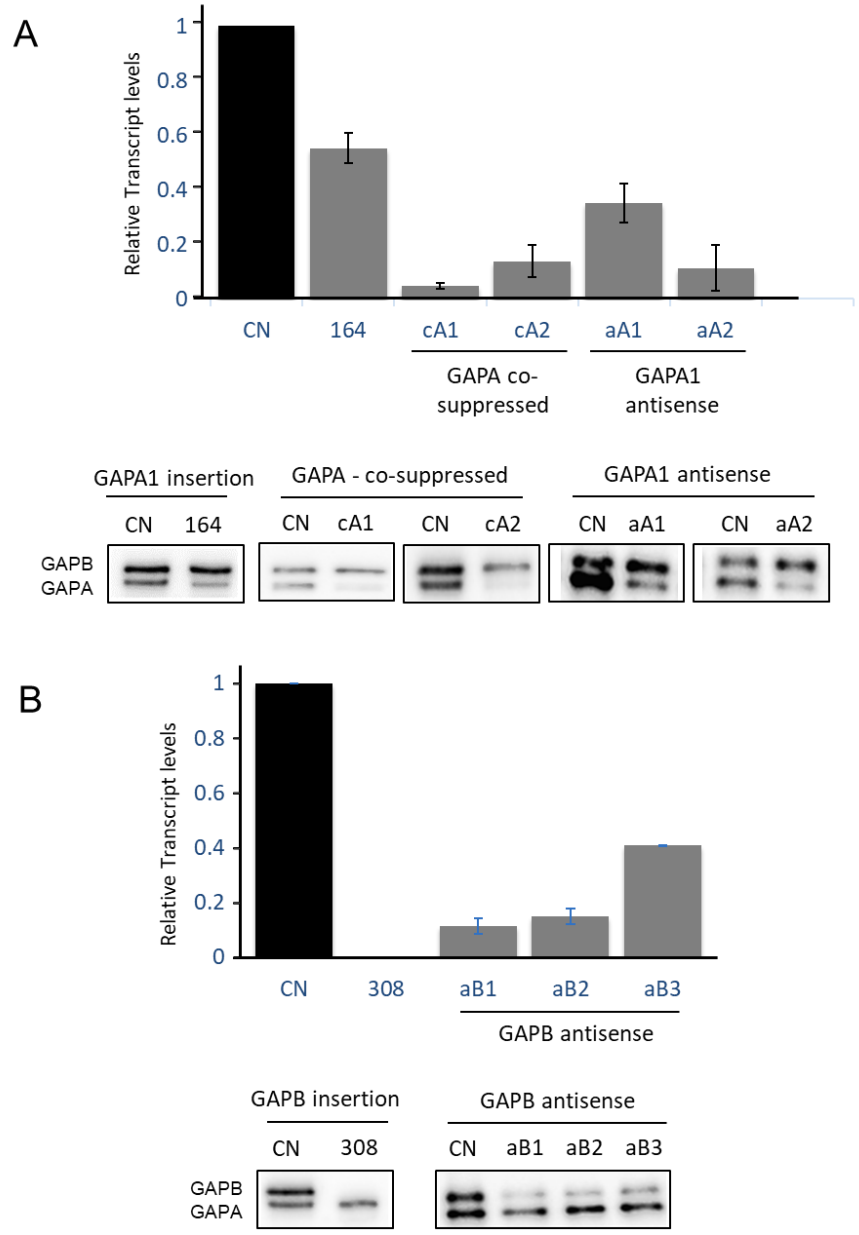

Figure 2. RT-qPCR and Immunoblot analysis of leaf proteins of wild type and experimental GAPDH plants. (A) Transcript and Protein levels in *gapa-1* (At3g26650; SAIL_164_D01), GAPA co-suppressed lines (cA), GAPA antisense lines (aA) and control (CN). (B) Transcript and Protein levels in *gapb* (At1g42970; SAIL_308_A06) and GAPB antisense lines (aB). Protein (6 µg) extracts from leaf discs taken from two leaves per plant and separated on a 12% acrylamide gel, transferred to membranes and probed with antibodies to GAPDH which recognises both GAPA and GAPB subunits. Error bars represent SE.

Figure 3

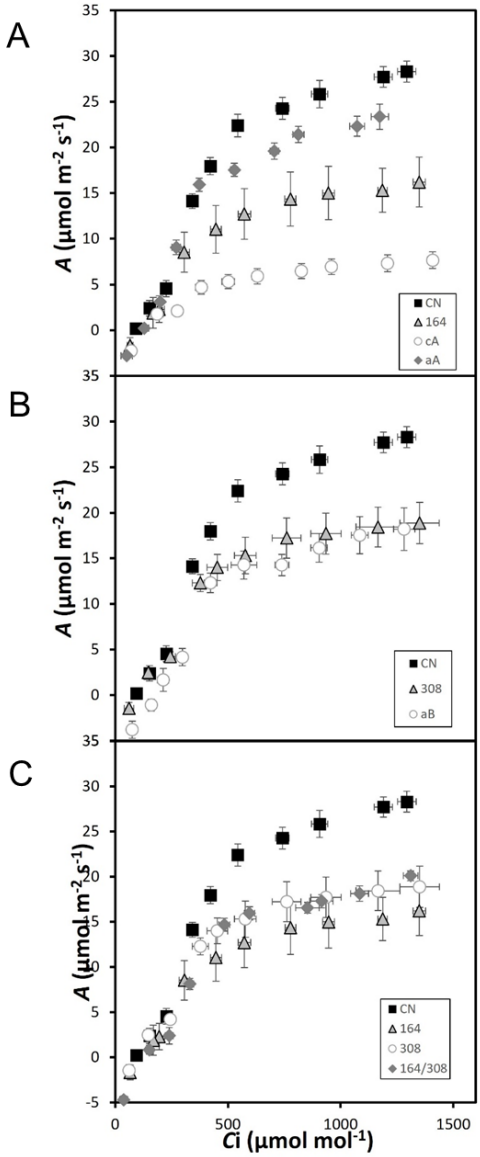

481
482
483 **Figure 3. Photosynthetic carbon fixation rate determined as a function of increasing CO_2**
484 **concentrations (*A*/*C*i) at saturating-light levels (1000 µmol m^{-2} s^{-1}).** (A) Controls (CN)
485 compared to *gapa-1* insertion line (164), GAPA co-suppressed (cA) and GAPA antisense (aA)
486 lines(. (B) CN compared to *gapb* insertion line (308) and GAPB antisense (aB) line lines and
487 (C) Photosynthetic carbon fixation of CN compared to single insertion mutants *gapa-1* (164)
488 and *gapb* (308) and the double mutant *gapa-1/gapb* (164/308). Extrapolated data are in Table
489 1. Error bars represent SE of 6 plants per line).
490

Figure 4

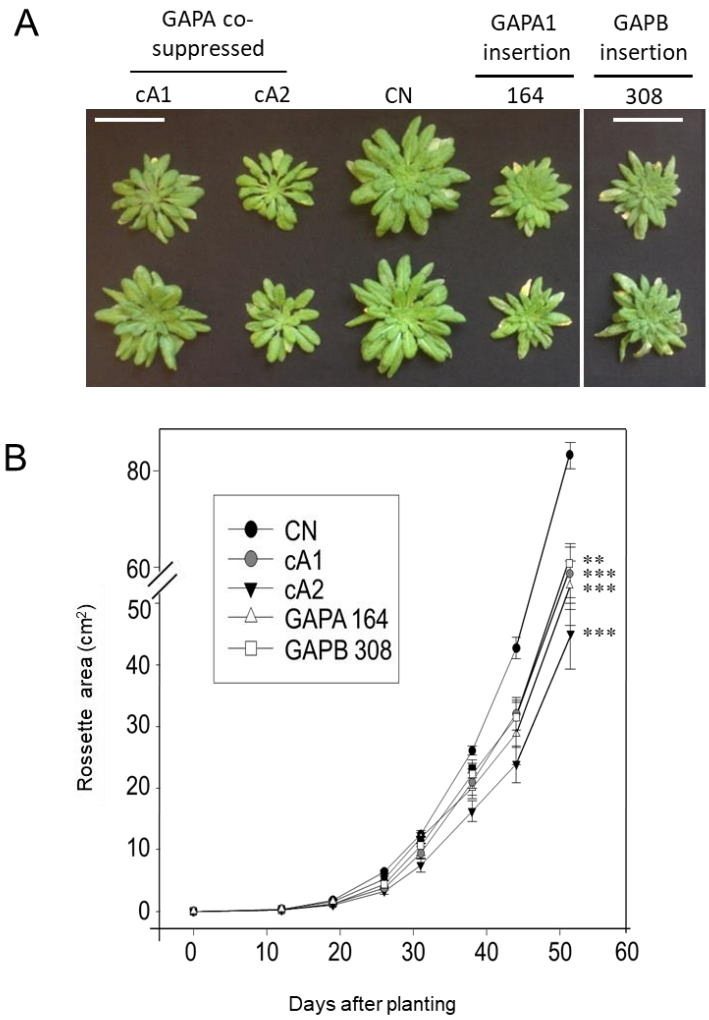

Figure 4. Growth analysis of control and experimental lines grown. (A) Plants were grown at 130 µmol m^{-2} s^{-1} light intensity in short days (8h/16h days) for 52 days. White bar represents a size of 6cm. (B) Plant growth rate evaluated over the first 52 days. Lines co-suppressing GAPA (cA), Controls (CN), *gapa-1* insertion mutant (164) and *gapb* insertion mutant (308) are represented. Results are representative of 9 to 12 plants per line (CN plants include azygous lines segregated from primary transformants). Data were statistically analysed using 2-way ANOVA. Significant differences * ($p<0.10$); **($p<0.05$); *** ($p<0.01$) are indicated. Unless indicated, results are presented as a percentage of CN (CN = 100%). Error bars represent SE.

Figure 5

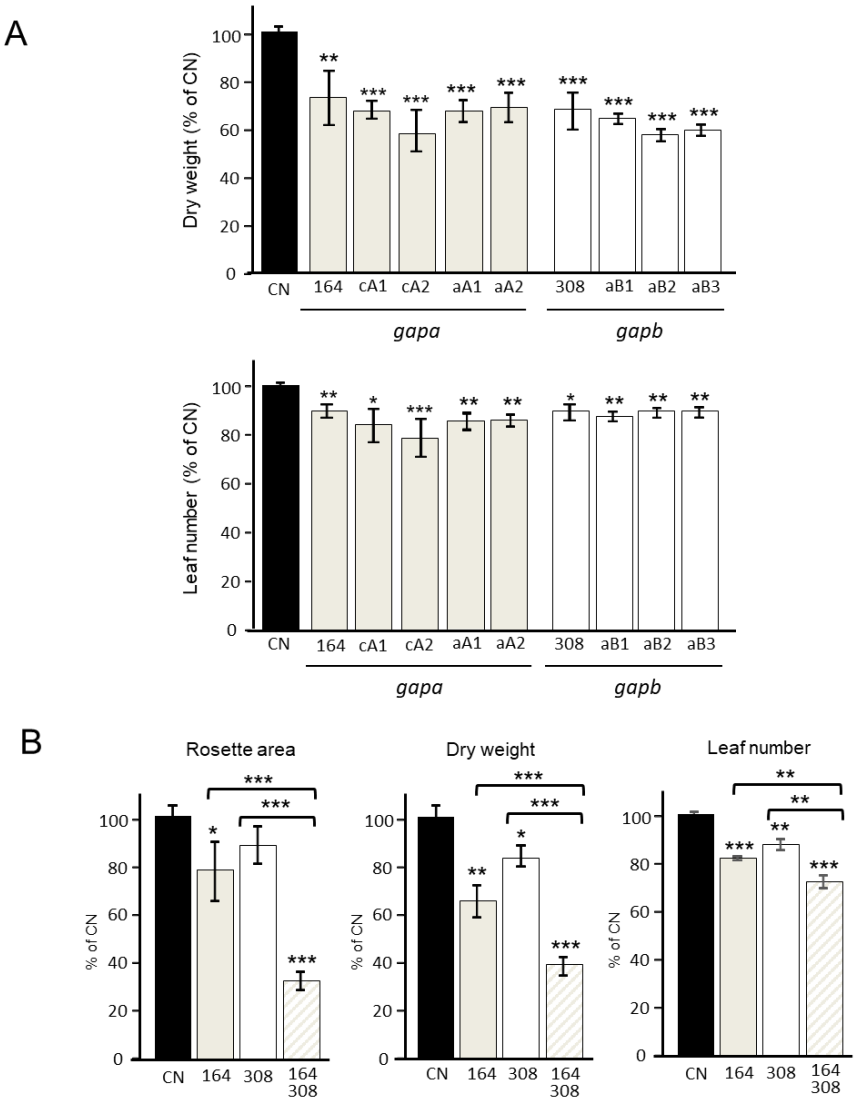

Figure 5. Growth analysis of control and experimental lines grown in low light. (A) *gapa-1* (164) and *gapb* (308) insertion mutants and GAPA co-suppressed (cA), GAPA antisense (aA) and GAPB (aB) antisense lines were analyzed in parallel. Results are representative of 8 plants per line. (B) *gapa-1* (164) and *gapb* (308) insertion mutants and the double mutant *gapa-1/gapb* (164/308) crosses were evaluated. Results are representative of 9 to 12 plants per line. Plants were grown at 130 µmol m^{-2} s^{-1} light intensity in short days for 46 days. (CN plants include azygous lines segregated from primary transformants). Data were statistically analysed using 2-way ANOVA. Significant differences * ($p<0.10$); **($p<0.05$); *** ($p<0.01$) are indicated. Results are presented as a percentage of CN (CN = 100%). Error bars represent SE.

514

515 References

516

517 **Baalmann E, Scheibe R, Cerff R, Martin W** (1996) Functional studies of chloroplast
518 glyceraldehyde-3-phosphate dehydrogenase subunits A and B expressed in *Escherichia*
519 *coli:* formation of highly active A4 and B4 homotetramers and evidence that
520 aggregation of the B4 complex is mediated by the B subunit carboxy terminus. Plant
521 Molecular Biology **32:** 505-513

522 **Baalmann E, Scheibe R, Cerff R, Martin W** (1996) Functional studies of chloroplast
523 glyceraldehyde-3-phosphate dehydrogenase subunits A and B expressed in Escherichia
524 coli: formation of highly active A4 and B4 homotetramers and evidence that
525 aggregation of the B4 complex is mediated by the B subunit carboxy terminus. Plant
526 Mol Biol **32:** 505-513

527 **Baker NR, Oxborough K, Lawson T, Morison JIL** (2001) High resolution imaging of
528 photosynthetic activities of tissues, cells and chloroplasts in leaves. Journal of
529 Experimental Botany **52:** 615-621

530 **Barbagallo RP, Oxborough K, Pallett KE, Baker NR** (2003) Rapid, noninvasive screening
531 for perturbations of metabolism and plant growth using chlorophyll fluorescence
532 imaging. Plant Physiology **132:** 485-493

533 **Bernacchi CJ, Singsaas EL, Pimentel C, Portis JAR, Long SP** (2001) Improved temperature
534 response functions for models of Rubisco-limited photosynthesis. Plant Cell and
535 Environment **24:** 253-260

536 **Burgess AJ, Masclaux-Daubresse C, Strittmatter G, Weber APM, Taylor SH, Harbinson**
537 **J, Yin X, Long S, Paul MJ, Westhoff P, Loreto F, Ceriotti A, Saltenis VLR, Pribil**
538 **M, Nacry P, Scharff LB, Jensen PE, Muller B, Cohan J-P, Foulkes J, Rogowsky**
539 **P, Debaeke P, Meyer C, Nelissen H, Inzé D, Klein Lankhorst R, Parry MAJ,**
540 **Murchie EH, Baekelandt A** (2022) Improving crop yield potential: Underlying
541 biological processes and future prospects. Food and Energy Security **n/a:** e435

542 **Carmo-Silva AE, Marri L, Sparla F, Salvucci ME** (2011) Isolation and compositional
543 analysis of a CP12-associated complex of calvin cycle enzymes from *Nicotiana*
544 *tabacum*. Protein and Peptide Letters **18:** 618-624

545 **Cerff R** (1979) Quaternary structure of higher plant glyceraldehyde-3-phosphate
546 dehydrogenases. Eur J Biochem **94:** 243-247

547 **Cerff R** (1995) The chimeric nature of nuclear genomes and the antiquity of introns as
548 demonstrated by the GAPDH gene system. Elsevier Science

549 **Clough SJ, Bent AF** (1998) Floral dip: a simplified method for Agrobacterium-mediated
550 transformation of Arabidopsis thaliana. Plant J **16:** 735-743

551 **Cséke C, Buchanan BB** (1986) Regulation of the formation and utilization of photosynthate
552 in leaves. Biochimica et Biophysica Acta - Reviews on Bioenergetics **853:** 43-63

553 **De Souza AP, Burgess SJ, Doran L, Hansen J, Manukyan L, Maryn N, Gotarkar D,**
554 **Leonelli L, Niyogi KK, Long SP** (2022) Soybean photosynthesis and crop yield are
555 improved by accelerating recovery from photoprotection. Science **377:** 851-854

556 **Driever SM, Simkin AJ, Alotaibi S, Fisk SJ, Madgwick PJ, Sparks CA, Jones HD, Lawson**
557 **T, Parry MAJ, Raines CA** (2017) Increased SBPase activity improves photosynthesis
558 and grain yield in wheat grown in greenhouse conditions. Philosophical Transactions
559 of the Royal Society B **372:** 1730

560 **Fermani S, Sparla F, Falini G, Martelli PL, Casadio R, Pupillo P, Ripamonti A, Trost P**
561 (2007) Molecular mechanism of thioredoxin regulation in photosynthetic A2B2-

562 glyceraldehyde-3-phosphate dehydrogenase. Proc Natl Acad Sci U S A **104:** 11109-
563 11114
564 **Fermani S, Sparla F, Falini G, Martelli PL, Casadio R, Pupillo P, Ripamonti A, Trost P**
565 (2007) Molecular mechanism of thioredoxin regulation in photosynthetic A2B2-
566 glyceraldehyde-3-phosphate dehydrogenase. Proceedings of the National Academy of
567 Sciences **104:** 11109-11114
568 **Harrison EP, Willingham NM, Lloyd JC, Raines CA** (1998) Reduced sedoheptulose-1,7-
569 bisphosphatase levels in transgenic tobacco lead to decreased photosynthetic capacity
570 and altered carbohydrate accumulation. Planta **204:** 27-36
571 **Howard TP, Lloyd JC, Raines CA** (2011) Inter-species variation in the oligomeric states of
572 the higher plant Calvin cycle enzymes glyceraldehyde-3-phosphate dehydrogenase and
573 phosphoribulokinase. Journal of Experimental Botany **62:** 3799-3805
574 **Howard TP, Metodiev M, Lloyd JC, Raines CA** (2008) Thioredoxin-mediated reversible
575 dissociation of a stromal multiprotein complex in response to changes in light
576 availability. Proceedings of the National Academy of Sciences **105:** 4056-4061
577 **Iadarola P, Zapponi MC, Ferri G** (1983) Molecular forms of chloroplast glyceraldehyde-3-
578 P-dehydrogenase. Experientia **39:** 50-52
579 **IPCC** (2014) Climate change 2014 impacts, adaptation and vulnerability: Part A: Global and
580 sectoral aspects: Working group II contribution to the fifth assessment report of the
581 intergovernmental panel on climate change. *In* VRB C. B. Field, D. J. Dokken, et al.,
582 eds, ed. Cambridge University Press, Cambridge, UK and New York, NY, USA
583 **IPCC** (2019) Summary for Policymakers. In:Climate change and land: an IPCC special report
584 on climate change, desertifcation, land degradation, sustainableland management, food
585 security, and greenhouse gas fuxes in terrestrial ecosystems. *In* PR Shukla, J Skea, E
586 Calvo Buendia, V Masson-Delmotte, HO Pörtner, DC Roberts, P Zhai, R Slade, S
587 Connors, R Van Diemen, M Ferrat, eds. Cambridge University Press, Cambridge, UK
588 and New York, NY, USA.
589 **Kubis A, Bar-Even A** (2019) Synthetic biology approaches for improving photosynthesis.
590 Journal of Experimental Botany **70:** 1425-1433
591 **Lawson T, Lefebvre S, Baker NR, Morison JIL, Raines CA** (2008) Reductions in mesophyll
592 and guard cell photosynthesis impact on the control of stomatal responses to light and
593 CO(2). Journal of Experimental Botany **59:** 3609-3619
594 **Le Quéré C, Raupach MR, Canadell JG, Marland G, Bopp L, Ciais P, Conway TJ, Doney**
595 **SC, Feely RA, Foster P, Friedlingstein P, Gurney K, Houghton RA, House JI,**
596 **Huntingford C, Levy PE, Lomas MR, Majkut J, Metzl N, Ometto JP, Peters GP,**
597 **Prentice IC, Randerson JT, Running SW, Sarmiento JL, Schuster U, Sitch S,**
598 **Takahashi T, Viovy N, van der Werf GR, Woodward FI** (2009) Trends in the
599 sources and sinks of carbon dioxide. Nature Geoscience **2:** 831-836
600 **Lopez-Calcagno PE, Abuzaid AO, Lawson T, Raines CA** (2017) Arabidopsis CP12 mutants
601 have reduced levels of phosphoribulokinase and impaired function of the Calvin-
602 Benson cycle. Journal of Experimental Botany **68:** 2285-2298
603 **Lopez-Calcagno PE, Howard TP, Raines CA** (2014) The CP12 protein family: a
604 thioredoxin-mediated metabolic switch? Frontiers in Plant Science **5:** 9
605 **Marri L, Trost P, Pupillo P, Sparla F** (2005) Reconstitution and properties of the
606 recombinant glyceraldehyde-3-phosphate dehydrogenase/CP12/phosphoribulokinase
607 supramolecular complex of Arabidopsis. Plant Physiology **139:** 1433-1443
608 **Nakagawa T, Kurose T, Hino T, Tanaka K, Kawamukai M, Niwa Y, Toyooka K,**
609 **Matsuoka K, Jinbo T, Kimura T** (2007) Development of series of gateway binary
610 vectors, pGWBs, for realizing efficient construction of fusion genes for plant
611 transformation. J Biosci Bioeng **104:** 34-41

NASA (2020) Global climate change: Vital signs of the planet. https://climate.nasa.gov/413ppmquotes *In*,

Oxborough K, Baker NR (2000) An evaluation of the potential triggers of photoinactivation of photosystem II in the context of a Stern–Volmer model for downregulation and the reversible radical pair equilibrium model. Philosophical Transactions of the Royal Society of London. Series B: Biological Sciences **355:** 1489-1498

Pereira LS (2017) Water, agriculture and food: Challenges and issues. Water Resources Management **31:** 2985-2999

Pohlmeyer K, Paap BK, Soll J, Wedel N (1996) CP12: A small nuclear-encoded chloroplast protein provides novel insights into higher-plant GAPDH evolution. Plant Molecular Biology Reporter **32:** 969-978

Price GD, Evans JR, von Caemmerer S, Yu JW, Badger MR (1995) Specific reduction of chloroplast glyceraldehyde-3-phosphate dehydrogenase activity by antisense RNA reduces CO_2 assimilation via a reduction in ribulose bisphosphate regeneration in transgenic tobacco plants. Planta **195:** 369-378

Raines CA (2022) Improving plant productivity by re-tuning the regeneration of RuBP in the Calvin–Benson–Bassham cycle. New Phytologist **236:** 350-356

Raines CA, Cavanagh AP, Simkin AJ (2022) Chapter 9. Improving carbon fixation. *In* A Ruban, E Murchie, C Foyer, eds, Photosynthesis in Action, Ed 1. Academic Press

Ruuska SA, Andrews TJ, Badger MR, Price GD, von Caemmerer S (2000) The role of chloroplast electron transport and metabolites in modulating rubisco activity in tobacco. Insights from transgenic plants with reduced amounts of cytochrome *b/f* complex or glyceraldehyde 3-phosphate dehydrogenase. Plant Physiology **122:** 491-504

Scagliarini S, Trost P, Pupillo P (1998) The non-regulatory isoform of NAD(P)-glyceraldehyde-3-phosphate dehydrogenase from spinach chloroplasts. Journal of Experimental Botany **49:** 1307-1315

Scheibe R, Baalmann E, Backhausen JE, Rak C, Vetter S (1996) C-terminal truncation of spinach chloroplast NAD(P)-dependent glyceraldehyde-3-phosphate dehydrogenase prevents inactivation and reaggregation. Biochim Biophys Acta **1296:** 228-234

Sharkey TD (2016) What gas exchange data can tell us about photosynthesis. Plant, Cell & Environment **39:** 1161-1163

Sharkey TD, Bernacchi CJ, Farquhar GD, Singsaas EL (2007) Fitting photosynthetic carbon dioxide response curves for C3 leaves. Plant Cell and Environment **30:** 1035-1040

Simkin AJ (2019) Genetic engineering for global food security: photosynthesis and biofortification. Plants **8:** 586

Simkin AJ, Lopez-Calcagno PE, Davey PA, Headland LR, Lawson T, Timm S, Bauwe H, Raines CA (2017) Simultaneous stimulation of sedoheptulose 1,7-bisphosphatase, fructose 1,6-bisphophate aldolase and the photorespiratory glycine decarboxylase H-protein increases CO_2 assimilation, vegetative biomass and seed yield in Arabidopsis. Plant Biotechnology Journal **15:** 805-816

Simkin AJ, Lopez-Calcagno PE, Raines CA (2019) Feeding the world: improving photosynthetic efficiency for sustainable crop production. Journal of Experimantal Botany **70:** 1119-1140

Simkin AJ, McAusland L, Lawson T, Raines CA (2017) Over-expression of the RieskeFeS protein increases electron transport rates and biomass yield. Plant Physiology **175:** 134-145

Sparla F, Pupillo P, Trost P (2002) The C-terminal extension of glyceraldehyde-3-phosphate dehydrogenase subunit B acts as an autoinhibitory domain regulated by thioredoxins

and nicotinamide adenine dinucleotide. Journal of Biological Chemistry **277:** 44946-44952

Sparla F, Zaffagnini M, Wedel N, Scheibe R, Pupillo P, Trost P (2005) Regulation of photosynthetic GAPDH dissected by mutants. Plant Physiology **138:** 2210-2219

Suzuki Y, Ishiyama K, Sugawara M, Suzuki Y, Kondo E, Takegahara-Tamakawa Y, Yoon D-K, Suganami M, Wada S, Miyake C, Makino A (2021) Overproduction of chloroplast glyceraldehyde-3-phosphate dehydrogenase improves photosynthesis slightly under elevated [CO_2] conditions in rice. Plant and Cell Physiology **62:** 156-165

Trost P, Fermani S, Marri L, Zaffagnini M, Falini G, Scagliarini S, Pupillo P, Sparla F (2006) Thioredoxin-dependent regulation of photosynthetic glyceraldehyde-3-phosphate dehydrogenase: autonomous vs. CP12-dependent mechanisms. Photosynthesis Research **89:** 263-275

von Caemmerer S, Farquhar GD (1981) Some relationships between the biochemistry of photosynthesis and the gas exchange of leaves. Planta **153:** 376-387

von Caemmerer S, Lawson T, Oxborough K, Baker NR, Andrews TJ, Raines CA (2004) Stomatal conductance does not correlate with photosynthetic capacity in transgenic tobacco with reduced amounts of Rubisco. J Exp Bot **55:** 1157-1166

Wolosiuk RA, Buchanan BB (1976) Studies on the regulation of chloroplast NADP-linked glyceraldehyde-3-phosphate dehydrogenase. The Journal of Biological Chemistry **251:** 6456-6461